

Buoyancy-Driven Heat and Mass Transfer in Magnetized Nanofluid with Dissipative Porous Media

Mohammed Modather Mohammed Abdou^{1,2,*} and Refah Mohammed Masfar Al-Witheh¹

¹Department of Mathematics, Prince Sattam Bin Abdulaziz University, Al Kharj, College of Science and Humanity Studies, 11942, Saudi Arabia

²Department of Mathematics, Aswan University, Faculty of Science, 81528, Aswan, Egypt

Received: 12 Jun. 2024, Revised: 4 Jul. 2024, Accepted: 7 Aug. 2024

Published online: 1 Jan. 2025

Abstract: A nanofluid of electrically conducting, viscous, incompressible Cu-water is being studied to determine the effect of Joule heating and viscous dissipation on its flow along a vertical surface. Despite the presence of suction/injection and velocity slip, the flow takes place in a porous medium that is non Darcian. Heat and mass transport in mixed convective boundary layer flow are considered in the study, along with the combined effects of buoyancy force and magneto-hydrodynamics (MHD). The governing partial differential equations were simplified into similarity boundary layer equations using appropriate transformations. After then, the equations were resolved by combining the shooting technique with the Runge-Kutta numerical integration method. Local skin friction coefficient, Nusselt number, Sherwood number, concentration, temperature, and velocity are all shown graphically, along with the effects of all flow parameters. Whether the fluid is being injected or suctioned, the results showed that a decrease in fluid temperature and concentration occurs when the thermal buoyancy ratio parameter Nr is increased. Nevertheless, as Nr rises, the fluid's velocity also increases.

Keywords: Nanofluids, velocity slip, viscous dissipation

1 Introduction

In recent years, nanotechnology has grown into a fascinating and influential area of study across many disciplines, including chemistry, engineering, physics, and more. Medicine, the military, IT, electronics, computer science, petrochemicals, biology, and many more fields stand to benefit greatly from this technology. Many scientists have been interested in studying the transmission of heat and mass in nonfluid materials because of this phenomenon [1, 2, 3, 4, 5, 6, 7]. Researchers Lee et al. [5] looked at how oxide nanoparticles in fluids affect thermal conductivity measurements. Nanofluids, a suspension of nanophase particles in a base liquid, were the subject of research by Xuan and Li [6]. Research on how nanofluids' transport properties and heat transfer performance are affected by suspended ultrafine particles was carried out by Xuan and Roetzel [7]. The results of this study show that nanofluids could greatly enhance heat transmission. Numerical research on the uniform free-stream flow of a nanofluid over a moving, semi-infinite flat plate was carried out by Bachok et al.

[8]. The problem of the flow of a nanofluid a combination of pure fluid and nanoparticles along a permeable vertical plate in the presence of a magnetic field has been studied by Chamkha and Aly [9]. This type of flow is defined by natural convection and boundary-layer effects. In their study, Khan and Pop [10] examined the boundary layer flow of a nanofluid across a stretching sheet. Research on the natural convective boundary-layer flow of nanofluids over a vertical plate was carried out by Kuznetsov and Nield [11].

There is a plethora of unique applications for transport processes in porous media, including thermal insulation, geothermal engineering, energy maintenance, grain storage devices, ceramic processes, chemical catalytic reactors, groundwater hydrology, cooling of electronic systems, and many more.

Natural convection over a horizontal plate in a porous medium saturated with a nanofluid was studied by Gorla and Chamkha [12] for heat and mass transfer boundary layer flow. A continuous, smooth, spontaneous convective boundary-layer flow over a penetrable vertical cone surrounded by a porous material filled with a nanofluid

* Corresponding author e-mail: m.modather@yahoo.com

was studied by Chamkha and Rashad [13]. The presence of a consistent side-to-side mass flow was also taken into account. The effect of a constant transpiration velocity on the non-Newtonian fluid's flow through a permeable vertical cone in a porous media saturated with a nanofluid was investigated by Rashad et al. [14]. Using the Brinkman-Forchheimer-Darcy extended model, Rashad [15] examined the flow of a boundary layer surrounding a sphere immersed in a porous medium containing a nanofluid.

According to Srinivasacharya [16], a porous medium containing nanofluid was used to study the natural convection on a sloping, wavelike surface. While studying the heat transfer and natural convection flow of nanofluids in a vertical rectangular duct that flows through a porous medium, Umavathi et al. [17] employed the Darcy-Forchheimer-Brinkman model. The mixed convection flow of a non-Newtonian fluid across a vertical surface saturated in a porous medium and filled with a nanofluid was studied by Rashad et al. [18]. Under convective boundary conditions, Rashad et al. [19] studied nanofluid flow through a horizontal circular cylinder immersed in a porous medium.

Due to its numerous real-world engineering and technological applications, magneto hydrodynamic (MHD) mixed convection heat transfer flow has garnered a lot of attention from the technical community. The list of these uses is long and includes things like magnetic energy extraction, plastic sheet manufacturing, cooling nuclear reactors, studying plasma, extracting geothermal energy, producing artificial fiber, and cooling underground electric cables.

Abdulkadhim et al. [20] investigated the effects of heat generation and heat absorption on the natural convection of a Cu-water nanofluid in a wavy enclosure subjected to a magnetic field. The researchers looked at the flow and heat transfer properties from different angles and made it more versatile for use in various engineering applications. They specifically looked at how the Hartmann number (Ha), Rayleigh number (Ra), and concentration of nanoparticles affected the process. For their numerical study, Medebber et al. [21] used magnetic fields to simulate natural convection in a vertical cylindrical annular chamber containing Cu-water nanofluid. The enclosure's top and bottom walls are thermally insulated, while the vertical walls are maintained at uniform hot and cold temperatures, TH and TC , respectively. Considering the effect of an induced magnetic field on the steady magnetohydrodynamics (MHD) stagnation-point flow of nanofluid over a stretching or shrinking sheet, Junoh et al. [22] investigated the modified Buongiorno's nanofluid model. Suction and zero mass flux were also considered in the research. The same authors [23] investigated in an earlier work how an artificially produced magnetic field affects the continuous two-dimensional flow of a non-compressible electrically conductive nanofluid, which happens as a result of an expanding or contracting

surface. The numerical investigation of the natural convection of an Al_2O_3 -water nanofluid in a vertically oriented annulus subjected to a uniform magnetic field was carried out by Berrahil et al. [24]. Using a Cu-water nanofluid, Das et al. [25] investigated how nanoparticles affected the flow and heat transfer characteristics across a stretched permeable sheet. A magnetic field, slip velocity, and thermal convective boundary conditions were all taken into account in the investigation. Forced convection between laminar flows of hot and cold nanofluids separated by a thin membrane in a horizontal channel was quantitatively analyzed by Raisi and Qanbary [26]. The outside surface of the channel walls is divided into two parts-NMP and MP-and is thermally insulated. The section of the channel that is not impacted by the magnetic field, running from the entrance to the middle, is called the non-magnetic portion (NMP). When subjected to a uniformly strong, perpendicular magnetic field, the channel wall spanning the channel's middle and exit sections is said to be MP. Within the context of non-isothermal and continuous heat flow conditions, Ferdows et al. [27] performed a numerical analysis to investigate the effects of an induced magnetic field on the hydrodynamics and thermal build-up of nanofluids including nanoparticles in water. The effect of an outside magnetic field on ferrofluid convection in a container with an elliptical heated cylinder was studied by Sheikholeslami et al. [28]. The hydrothermal behavior of the system was investigated in relation to the Rayleigh and Hartmann numbers, the volume fraction of Fe_3O_4 , and other parameters. The interaction between a heated viscous incompressible magnetic nanofluid and a cold wall was numerically analyzed by Hriczó [29]. The interaction occurred in the presence of a spatially variable magnetic field. Using a nanofluid, Sheikholeslami and Ganji [30] investigated how fluid flow and heat transfer behave under a continuous magnetic field. Using a variable magnetic field, the same authors [31] investigated nanofluid flow and heat transmission. A study was carried out experimentally by Sun et al. [32] to examine the flow characteristics and heat transfer of magnetic nanofluids composed of Fe_3O_4 and water in a magnetic field. A magnetic flux density distribution was used to integrate the experimental data. The effects of the field gradient, different orientations of the magnetic field, and the magnetic flux density on the local Nusselt number and flow pressure decrease were examined. Laminar convection in a horizontal cylindrical enclosure heated from below was the subject of an analytical and numerical examination by Krakov and Nikiforov [33]. It was found in their investigation that a homogeneous external magnetic field can impact gravity convection or cause instability in the equilibrium state of the magnetic nanofluid. In their investigation of the convective heat transfer of a magnetic nanofluid (MNF) within a square enclosure subjected to uniform magnetic fields, Hajiyan et al. [34] take into account the nonlinearity of the thermal conductivity, which is dependent on the magnetic field.

Joule heating is the process by which electrons in conduction transfer to atoms in conductors through collisions, and energy viscous dissipation is the work done by velocity in opposing viscous tension. Important considerations that come up when a plate is heated or cooled include viscous dissipation and Joule heating. These phenomena are widely used in many different processes, including food processing, electronic cigarette manufacturing, electricity generation, and the cooling of metallic sheets.

The effect of viscosity and joules dissipation on magneto hydrodynamic flow across a porous surface immersed in a porous medium was investigated by Devi and Ganga [35]. The influence of viscous and ohmic dissipations on a continuous two-dimensional radiative magnetohydrodynamic (MHD) boundary-layer flow of an electrically conducting nanofluid across a vertical plate was investigated in a study by Ganga et al. [36]. The researchers looked at internal heat generation/absorption as well as other potential effects. Water, an electrically conducting nanofluid, was studied by Mabood et al. [37] to determine the effects of magnetohydrodynamic (MHD) laminar boundary layer flow on mass and heat transmission. This flow considered viscous dissipation and happened across a nonlinear stretching sheet. In their study, Hayat et al. [38] investigated how a Cu-water nanofluid with viscous dissipation and Joule heating flows over a stretched sheet in a magnetohydrodynamic (MHD) boundary layer when the melting heat transfer is not uniform. In their study, Pandey and Kumar [39] examined the effects of viscous dissipation and suction/injection on the magnetohydrodynamic (MHD) flow of a nanofluid through a convective-surfaced wedge, taking into account the conditions of slip flow and porous media. For their study on the flow of magneto-hydrodynamics (MHD) nanofluid along an exponentially stretched sheet, Besthapu et al. [40] considered the effects of thermal and solutal stratification, as well as mixed convection and viscous dissipation, in order to determine the thermal conductivity. In their study, Upreti et al. [41] investigated how heat generation/absorption and suction/injection behaved in conjunction to affect the magnetohydrodynamic (MHD) flow of a nanofluid containing silver (Ag) particles in water. This flow passed through a flat plate that was stretched in a porous medium. The study also took into account the loss of electrical energy caused by the viscosity and resistance of the flow. For their theoretical study, Gopal et al. [42] used an exponential stretching sheet to model the effects of viscosity dissipation, first-order chemical reactions, and ohmic effects on MHD nanofluid flow. The influence of mass suction and convective circumstances on the flow of a nanofluid with aligned magneto-hydrodynamics (MHD) slip was studied by Khan et al. [43]. Joule heating, viscous dissipation, and heat generation/absorption were considered. In an annular duct, electrically conducting magnetohydrodynamic (MHD) power law fluid flow was studied by Ahmed et al. [44] to determine the effect of

viscous dissipation and Joule heating on the forced convection heat transfer rate. Magnetohydrodynamics (MHD) flow and heat transfer over a stretching sheet in a porous material were studied by Swain et al. [45] in relation to viscous dissipation and Joule heating. The computational analysis performed by Khan et al. [46] examined the flow behavior and heat transfer properties of nanofluids containing silver nanoparticles in water. The convective stretching/shrinking of a cylinder around the stagnation point was studied in terms of magnetic field, heat generation/absorption, surface convection, and slip velocity, with viscous dissipation considered.

The effects of mixed convection on the mass and heat transfer in a Cu-water nanofluid's boundary layer flow across a vertical surface are examined in this work. Joule heating and viscous dissipation are considered. The analysis takes into account the scenarios of injection and suction via a porous media, the existence of a magnetic field, and velocity slip. The partial differential equations were converted to ordinary differential equations by using transformations without dimensions. After that, the effect of various factors on concentration, temperature, and velocity was examined by numerically solving these equations. We also looked at the local Sherwood number, Nusselt number, and skin friction coefficient. There is a high degree of consistency between the results and previous studies.

2 Mathematical Formation

The problem under consideration involves the study of a laminar boundary layer flow in a two-dimensional domain. The flow is driven by a combination of buoyancy forces and forced convection and is characterized by the presence of a magnetic field perpendicular to a heated vertical porous plate. The fluid being considered is a regular, electrically conducting, viscous, and incompressible nanofluid consisting of water with the addition of copper (Cu) nanoparticles. The plate is embedded in a porous medium, and the effect of slip, which is a first-order phenomenon, is considered. The slip directly influences the velocity of the flow. The flow is considered to be in the x -direction, moving upward along the plate, while the y -axis is perpendicular to it, as depicted in Figure 1. There exists a velocity, $v_0(x)$, that is perpendicular to the plate and is responsible for suction and injection. The surface is maintained at a consistent temperature T_w and a constant concentration of nanoparticles C_w . The ambient temperature far from the surface is denoted as T_∞ , and the concentration of nanoparticles far from the surface is denoted as C_∞ . It is assumed that T_∞ and C_∞ are uniform, with T_w being greater than T_∞ and C_w being greater than C_∞ .

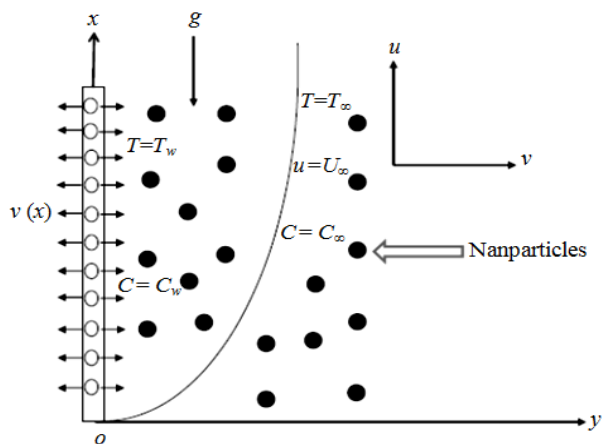


Fig. 1: Physical model and coordinate system

The equations regulating the conservation of mass, momentum, thermal energy, and concentration can be expressed under the assumptions and utilization of the Oberbeck-Boussinesq approximation:

$$\frac{\partial u}{\partial x} + \frac{\partial v}{\partial y} = 0, \quad (1)$$

$$u \frac{\partial u}{\partial x} + v \frac{\partial v}{\partial y} = \frac{\mu_{nf}}{\rho_{nf}} \frac{\partial^2 u}{\partial y^2} + \frac{g}{\rho_{nf}} [(\rho \beta_T)_{nf} (T - T_\infty) + (\rho \beta_C)_{nf} (C - C_\infty)] - \frac{\mu_{nf}}{\rho_{nf}} \frac{1}{K} (u - U_\infty) - \frac{\sigma_{nf} B_0^2}{\rho_{nf}} (u - U_\infty), \quad (2)$$

$$u \frac{\partial T}{\partial x} + v \frac{\partial T}{\partial y} = \left(\frac{k_{nf}}{(\rho C_p)_{nf}} \right) \frac{\partial^2 T}{\partial y^2} + \tau \left\{ D_B \frac{\partial C}{\partial y} \frac{\partial T}{\partial y} + \left(\frac{D_T}{T_\infty} \right) \left[\left(\frac{\partial T}{\partial y} \right)^2 \right] \right\} + \frac{\mu_{nf}}{(\rho C_p)_{nf}} \left(\frac{\partial u}{\partial y} \right)^2 + \frac{\sigma_{nf}}{(\rho C_p)_{nf}} u^2, \quad (3)$$

$$u \frac{\partial C}{\partial x} + v \frac{\partial C}{\partial y} = D_B \left(\frac{\partial^2 C}{\partial y^2} \right) + \left(\frac{D_T}{T_\infty} \right) \left(\frac{\partial^2 T}{\partial y^2} \right). \quad (4)$$

with the boundary conditions:

$$y = 0: u = N_1 \frac{\partial u}{\partial y}, v = v_0(x), T = T_w, C = C_w \quad (5)$$

$$y \rightarrow \infty: u = U_\infty, T = T_\infty, C = C_\infty,$$

where u and v denote the velocity components along the x -axis and y -axis respectively, B_0 represents the strength of the magnetic field, K is the permeability of the porous medium, D_B is the Brownian diffusion coefficient, μ_{bf} is the dynamic viscosity of the fluid, ρ_{bf} is the density of

the base fluid, μ_{nf} is the dynamic viscosity of the nanofluid, ρ_{nf} is the density of the nanofluid, k_{nf} represents the thermal conductivity, $(\rho C_p)_{nf}$ is the heat capacity of the fluid, and α_{nf} is the thermal diffusivity of the nanofluid, N_1 is the Navier slip coefficient, where $N_1 = 0$ indicates no-slip condition and $(\beta_C)_{nf}$ represents the coefficient of nanofluid concentration expansion, which is approximated by [47],

$$(\beta_C)_{nf} = \frac{1}{\rho_0} \frac{\partial \rho}{\partial C} \Big|_{T_0, P_0} \approx \frac{1}{\rho_f} \frac{\rho_s - \rho_f}{1 - C_\infty}.$$

where ρ_0 represents the density at a specific reference point, T_0 represents the temperature at the same reference point, and P_0 represents the pressure at the reference point.

The properties of the nanoparticles and based fluid is given by:

$$\left. \begin{aligned} \rho_{nf} &= (1 - \phi) \rho_{bf} + \phi \rho_{sp}, \\ \alpha_{nf} &= \frac{k_{nf}}{(\rho C_p)_{nf}}, \\ (\rho C_p)_{nf} &= (1 - \phi) (\rho C_p)_{bf} + \phi (\rho C_p)_{sp}, \\ (\rho \beta_T)_{nf} &= (1 - \phi) \rho_{bf} (\beta_T)_{bf} + \phi \rho_{sp} (\beta_T)_{sp}, \\ \frac{k_{nf}}{k_{bf}} &= \left[\frac{(k_{sp} + 2k_{bf}) + 2(k_{sp} - k_{bf})\phi}{(k_{sp} + 2k_{bf}) - (k_{sp} - k_{bf})\phi} \right], \\ \mu_{nf} &= \frac{\mu_{bf}}{(1 - \phi)^{2.5}}, \\ \frac{\sigma_{nf}}{\sigma_{bf}} &= \left[\frac{(\sigma_{sp} + 2\sigma_{bf}) + 2(\sigma_{sp} - \sigma_{bf})\phi}{(\sigma_{sp} + 2\sigma_{bf}) - (\sigma_{sp} - \sigma_{bf})\phi} \right], \end{aligned} \right\} \quad (6)$$

Here the lower indicate bf , sp and nf represent the fluid, the solid nanoparticles and the nanofluid respectively, C_p represents the specific heat at fixed pressure, B_T represents the coefficient of thermal expansion and ϕ is the solid nanoparticles volume fraction. Presenting the subsequent dimensionless quantities

$$\eta = y \sqrt{\frac{U_\infty}{\nu_{bf} x}},$$

$$\psi(x, y) = \sqrt{\nu_{bf} U_\infty x} f(\eta)$$

$$\theta = (T - T_\infty) / (T_w - T_\infty),$$

$$\chi = (C - C_\infty) / (C_w - C_\infty). \quad (7)$$

where ψ is the stream function and is denoted by:

$$u = \frac{\partial \psi}{\partial y}, \quad v = -\frac{\partial \psi}{\partial x}. \quad (8)$$

Equations (2-4) are transformed with the boundary conditions Equation (5) into the following ordinary differential equations

$$f''' + A_1 \left[\frac{1}{2} f f'' + \lambda \chi - \frac{f' - 1}{Da} \right] - A_2 M (f' - 1) + A_3 Nr \theta = 0, \tag{9}$$

$$\frac{k_{nf}}{k_{bf}} \theta'' + A_4 \left[Nb \theta' \phi' + Nt \theta'^2 + \frac{1}{2} Pr f \theta' \right] + Ec f''^2 + A_2 MEc f'^2 = 0, \tag{10}$$

$$\chi'' + \frac{1}{2} Sc f \chi' + \frac{Nt}{Nb} \theta'' = 0, \tag{11}$$

where dashes mean differentiation with respect to η with the boundary conditions:

$$\eta = 0: f = f_w, f' = \delta f''(0), \theta = 1, \chi = 1$$

$$\eta \rightarrow \infty: f' = 1, \theta = 0, \chi = 0. \tag{12}$$

The dimensionless variables used in Equations (9)-(12) are defined as:

$$Gr_{Tx} = x^3 g \beta_T (T_w - T_\infty) / \nu_{bf}^2, \quad Re_x = \frac{U_\infty x}{\nu_{bf}},$$

$$Nr = \frac{x g \beta_T (T_w - T_\infty)}{\rho_{bf} U_\infty^2} = \frac{Gr_{Tx}}{Re_x^2},$$

$$\lambda = \frac{x g \beta_C (C_w - C_\infty)}{\rho_{bf} U_\infty^2} = \frac{Gr_{Cx}}{Re_x^2}, \quad Pr = \frac{\nu_{bf}}{\alpha_{bf}},$$

$$Sc = \frac{\nu_{bf}}{D_B}, \quad Da = \frac{K U_\infty}{\nu_{bf} x}, \quad Nt = \frac{\tau_{DT} \nu_{bf}^2 (T_w - T_\infty)}{\alpha_{bf} T_\infty},$$

$$Nb = \frac{\tau_{DB} (C_w - C_\infty)}{\alpha_{bf} T_\infty}, \quad f_w = -2\nu_0(x) \sqrt{x/\nu_f U_\infty},$$

$$\delta = N_1 \sqrt{\frac{U_\infty}{\nu_{bf} x}}, \quad Ec = \frac{\mu_{bf} U_\infty^2}{k_{bf} (T_w - T_\infty)},$$

$$M = \frac{\sigma_{bf} B_0^2 x}{\rho_{bf} U_\infty},$$

$$A_1 = (1 - \phi)^{2.5} \left[1 - \phi + \phi \left(\frac{\rho_{sp}}{\rho_{bf}} \right) \right],$$

$$A_2 = (1 - \phi)^{2.5} \left[\frac{(\sigma_{sp} + 2\sigma_{bf}) + 2(\sigma_{sp} - \sigma_{bf})\phi}{(\sigma_{sp} + 2\sigma_{bf}) - (\sigma_{sp} - \sigma_{bf})\phi} \right],$$

$$A_3 = (1 - \phi)^{2.5} \left[1 - \phi + \phi \left(\frac{\rho \beta^*}{\rho \beta^*}_{sp} \right) \right],$$

$$A_4 = \left[1 - \phi + \phi \left(\frac{\rho C_p}{\rho C_p} \right)_{sp} \right]. \tag{13}$$

The symbol λ represents the solutal buoyancy ratio parameter. The Grashof number is denoted as Gr_x , the Reynolds number as Re_x , the Prandtl number as Pr , the Schmidt number as Sc , the buoyancy ratio parameter as Nr , the thermophoresis parameter as Nt , the Brownian motion parameter as Nb , the Darcy number parameter as

Da , the magnetic field parameter as M , the slip parameter as δ , and the suction/injection velocity at the plate as f_w . In the suction case, $f_w > 0$, while in the injection case, $f_w < 0$.

The physical parameters of primary interest in practical applications are the local skin-friction coefficient C_f , local Nusselt number Nu_x , and local Sherwood number Sh_x . The following can be described as:

$$C_f = \frac{\tau_w}{\rho_{bf} U_\infty^2}, \quad Nu_x = \frac{x}{k_{bf} (T_w - T_\infty)} q_w,$$

$$Sh_x = \frac{x}{D_B (C_w - C_\infty)} q_c, \tag{14}$$

where

$$\tau_w = \left(\mu_{nf} \frac{\partial u}{\partial y} \right)_{y=0}, \quad q_w = -k_{nf} \left(\frac{\partial T}{\partial y} \right)_{y=0},$$

$$q_c = -D_B \left(\frac{\partial C}{\partial y} \right)_{y=0}. \tag{15}$$

which are obtained as:

$$C_f Re_x^{-\frac{1}{2}} = f''(0), \quad Nu_x Re_x^{-\frac{1}{2}} = -\theta'(0),$$

$$Sh_x Re_x^{-\frac{1}{2}} = -\chi'(0), \tag{16}$$

where $Re_x = \frac{U_\infty x}{\nu_{bf}}$.

3 Numerical Method

The governing flow equations are transformed into ordinary differential equations through the application of scaling transforms. The Runge-Kutta Fehlberg numerical method was implemented in MATLAB to solve ordinary differential equations using the computational methodology known as the shooting technique. This approach involves transforming the system of nonlinear equations into a first-order ordinary differential equation (ODE) by inserting specific variables. The precision of the solutions is fine-tuned to the magnitude of 10^{-6} and the step size is set to 0.001.

Table 1: Thermo-physical properties of water and nanoparticle (Cu).

Property	Pure water	Cooper (Cu)
ρ (k g m ⁻³)	997.1	8933
C p (J k g ⁻¹ K ⁻¹)	4179	385
k (W m ⁻¹ K ⁻¹)	0.613	400
β_T (K ⁻¹)	21×10^{-5}	1.67
σ (S/m)	0.05	59.6×10^6

The following variables transform the Equations (9)-(12) into initial value problem:

$$\begin{aligned} h(1) &= f, & h(2) &= f', & h(3) &= f'', & hh1 &= f''', \\ h(4) &= \theta, & h(5) &= \theta', & hh2 &= \theta'', & h(6) &= \chi, \\ h(7) &= \chi', & hh3 &= \chi'', & & & & \end{aligned}$$

we define the following parameters

$$\begin{aligned} A_1 &= (1 - \phi)^{2.5} \left[1 - \phi + \phi \left(\frac{\rho_{sp}}{\rho_{bf}} \right) \right], \\ A_2 &= (1 - \phi)^{2.5} \left[\frac{(\sigma_{sp} + 2\sigma_{bf}) + 2(\sigma_{sp} - \sigma_{bf})\phi}{(\sigma_{sp} + 2\sigma_{bf}) - (\sigma_{sp} - \sigma_{bf})\phi} \right], \\ A_3 &= (1 - \phi)^{2.5} \left[1 - \phi + \phi \frac{(\rho\beta^*)_{sp}}{(\rho\beta^*)_{bf}} \right], \\ A_4 &= \left[1 - \phi + \phi \frac{(\rho C_p)_{sp}}{(\rho C_p)_{bf}} \right]. \end{aligned}$$

and

$$A_5 = \frac{k_{nf}}{k_{bf}} = \left[\frac{(k_{sp} + 2k_{bf}) + 2(k_{sp} - k_{bf})\phi}{(k_{sp} + 2k_{bf}) - (k_{sp} - k_{bf})\phi} \right].$$

The problem of the converted initial value appears in the formula:

$$\begin{aligned} hh1 &= -A_1 \left[0.5h(1)h(3) + \lambda h(6) - \frac{(h(2) - 1)}{Da} \right] \\ &+ A_2 M(h(2) - 1) - A_3 N r h(4), \end{aligned} \quad (17)$$

$$\begin{aligned} hh2 &= -\frac{1}{A_5} [A_4 (N b h(5) h(7) + N t h(5) + 0.5 P r h(1) h(5)) \\ &+ E c h(3) h(3) + A_2 M E c h(2) h(2)], \end{aligned} \quad (18)$$

$$hh3 = -0.5 S c h(1) h(7) - \frac{N t}{N b} h h 2, \quad (19)$$

with the boundary conditions:

$$\begin{aligned} \text{at } \eta = 0 & \quad h(1) = f_w, \quad h(2) = \delta h(3), \\ h(4) &= 1, \quad h(6) = 1, \\ \text{as } \eta \rightarrow \infty & \quad h(2) = 1, \quad h(4) = 0, \quad h(6) = 0. \end{aligned} \quad (20)$$

To verify the precision of the numerical findings, they have been verified with previously published research to ensure a strong level of concordance.

In Table 2, we compare the findings of the local Nusselt number $(-\theta'(0))$ obtained for different values of $Pr = 0.733, 1.0,$ and $, Da = \infty, f_w = Nt = Nr = Nb = \phi = \lambda = M = Ec = \delta = 0.0,$ with the results provided by Lin and Lin [48], Yih [49], Chamkha et al. [50], Nield and Kuznetsov [51,52], Aydın and Kaya [55] and Nabwey et al. [56].

The local Nusselt number $(-\theta'(0))$ obtained for $Pr = 0.733, 1.0,$ and $Da = \infty, f_w = Nt = Nr = Nb = \phi = \lambda =$

$M = Ec = \delta = 0.0$ in Table 3 is compared with the values reported by Yih [49], Chamkha et al. [50], Watanabe and Pop [54], Aydın and Kaya [55] and Nabwey et al. [56].

Table 4 presents a comparison of local Nusselt number $(-\theta'(0))$ results with those provided by Saeid [53], Aydın and Kaya [55] and Nabwey et al. [56] for various Pr and Nr values, while $Da = \infty, f_w = Nt = Nb = \phi = \lambda = M = Ec = \delta = 0.0.$

Table 2: Comparison of the values local Nusselt number $(-\theta'(0))$ for various values of Pr at $Da = \infty, f_w = Nt = Nr = Nb = \phi = \lambda = M = Ec = \delta = 0.0$

Pr	0.1	1.0	10.0
Lin & Lin [48]	0.140032	0.332057	0.728148
Yih [49]	0.140034	0.332057	0.728141
Chamkha et al. [50]	0.142003	0.332173	0.728310
Nield & Kuznetsove [51,52]	0.1580	0.3320	0.7300
Aydm & Kaya [55]	0.148123	0.332000	0.727801
Nabwey et al. [56]	0.159391	0.332059	0.728142
Present result	0.1593905	0.3320591	0.7281422

Table 3: Comparison of the values local Nusselt number $(-\theta'(0))$ for various values Pr with $Da = \infty, f_w = Nt = Nb = Nr = \lambda = \phi = M = Ec = \delta = 0.0$

Pr	0.733	1.0
Yih [49]	0.297526	0.332057
Chamkha et al. [50]	0.29760	0.33217
Watanabe and Pop [54]	0.29755	0.33206
Aydom amd Kaua [55]	0.29753	0.33206
Nabawey et al. [56]	0.297546	0.332059
Present result	0.2975463	0.3320591

Table 4: Comparison of the values local Nusselt number $(-\theta'(0))$ for various values Pr and Nr at $Da = \infty, f_w = Nt = Nb = \lambda = \phi = M = Ec = \delta = 0.0$

	Saeid [53]	Aydm & Kaya [55]	Nabwey et al. [56]	Present result
Nr	$Pr = 0.72$			
0.0	0.309	0.297	0.296	0.295659
0.2	0.332	0.332	0.332	0.331525
0.4	0.361	0.356	0.356	0.356122
0.6	0.382	0.376	0.376	0.375477
0.8	0.402	0.392	0.392	0.391684
1.0	0.416	0.406	0.406	0.405753
Nr	$Pr = 0.70$			
0.0	0.628	0.646	0.646	0.645923
0.2	0.698	0.698	0.699	0.698603
0.4	0.752	0.740	0.739	0.739339
0.6	0.791	0.772	0.773	0.773147
0.8	0.822	0.802	0.802	0.802334
1.0	0.851	0.827	0.828	0.828183

4 Results and Discussions

A number of characteristics, including as concentration, local skin friction coefficient, local Nusselt number, and

local Sherwood number, as well as velocity, temperature, and concentration, are shown graphically to illustrate their effects on flow. Multiple values of the following parameters were calculated: nanoparticle volume fraction (ϕ),

Darcy number (Da), magnetic field (M), Eckert number (Ec), Brownian motion (Nb), Lewis number (Nt), thermal buoyancy ratio (Nr), and velocity slip (δ).

The effects of the nano particle's volume fraction parameter ϕ on the velocity, temperature, and concentration profiles are shown in Figures 2, 3, 4. Both the fluid's temperature and concentration are shown to increase when the volume fraction parameter ϕ rises, as is evident from the figures. Whatever the case may be, it always causes the fluid's velocity to decrease, whether the suction or injection is constant.

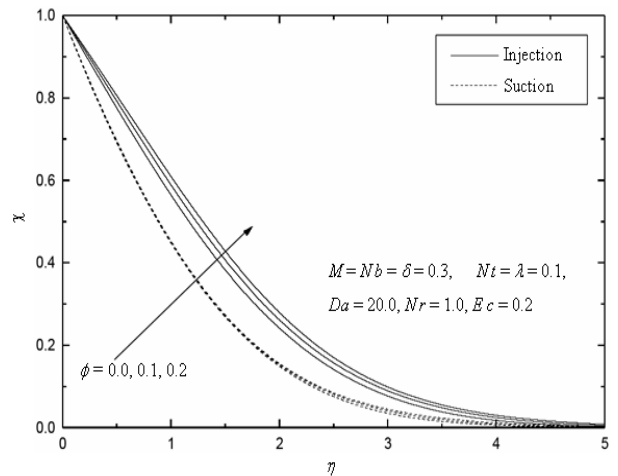


Fig. 4: Concentration profiles for various values of volume fraction parameter ϕ

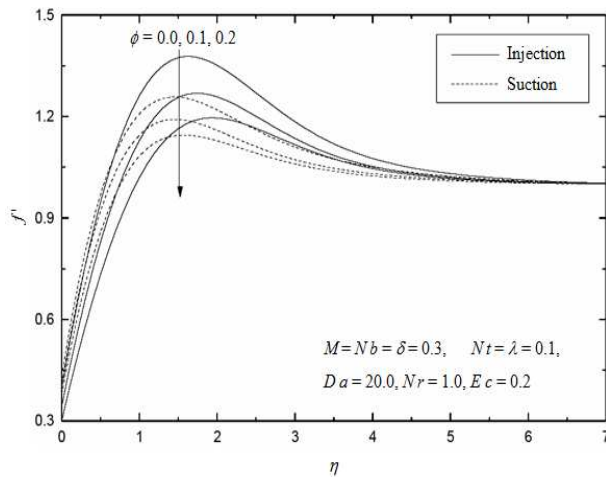


Fig. 2: Velocity profiles for various values of volume fraction parameter ϕ

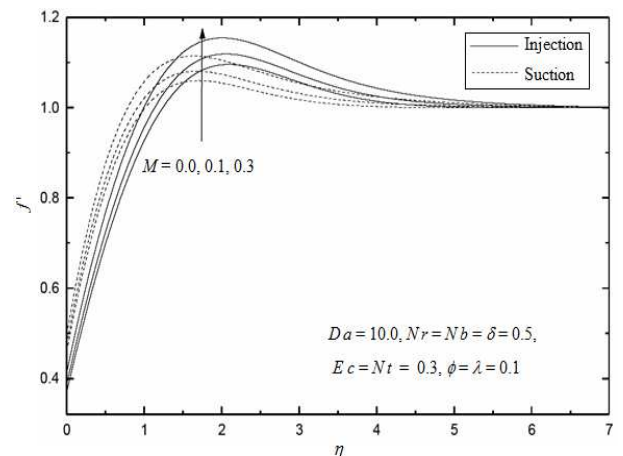


Fig. 5: Velocity profiles for various values of magnetic field parameter M

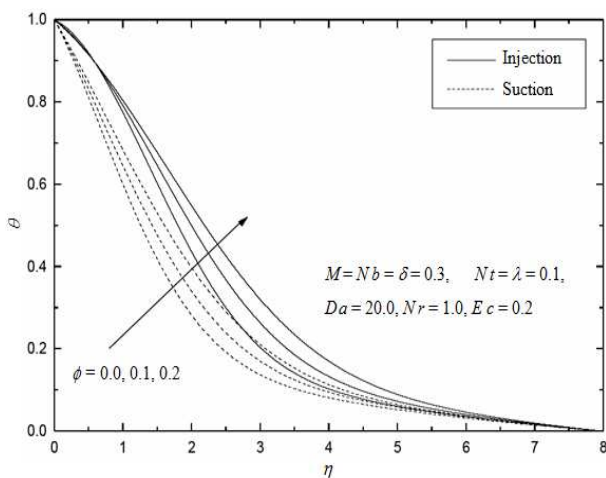


Fig. 3: Temperature profiles for various values of volume fraction parameter ϕ

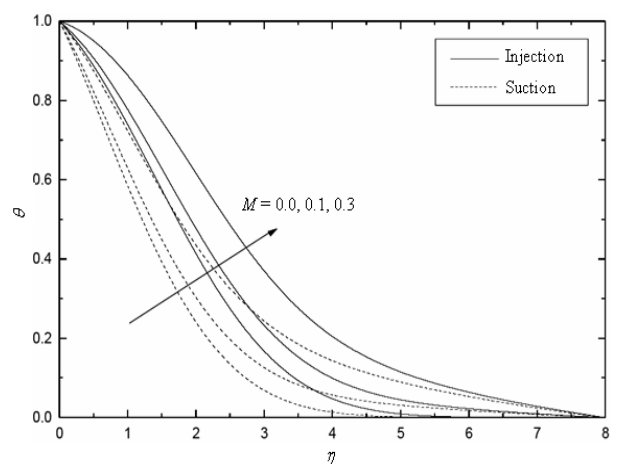


Fig. 6: Temperature profiles for various values of magnetic field parameter M

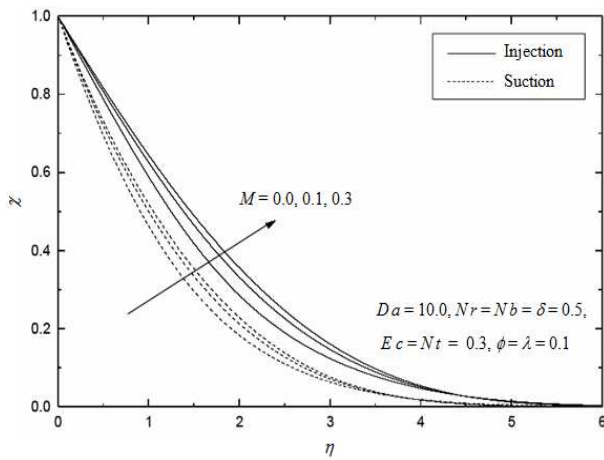


Fig. 7: Concentration profiles for various values of magnetic field parameter M

Figures 5, 6, 7 show how the velocity, temperature, and concentration profiles are affected by the magnetic field parameter M . Increasing the magnetic field parameter M causes the fluid velocity and temperature to rise, as shown in these figures. Nevertheless, it triggers a drop in fluid concentration and dampens the temperature and velocity increases brought about by Lorentz forces generated by a magnetic field. As a result of these forces, the fluid's concentration drops and its velocity and temperature rise. Injection and suction scenarios are identical in this regard.

Figures 8, 9, 10 show how the local skin friction coefficient, local Nusselt number, and local Sherwood number are affected by the Darcy number (Da) and the magnetic field parameter (M). The figures show that the local skin friction coefficient, local Nusselt number, and local Sherwood number all drop as the Darcy number (Da) increases. The decrease in porosity of the porous medium causes an increase in confinement, which in turn causes this reduction.

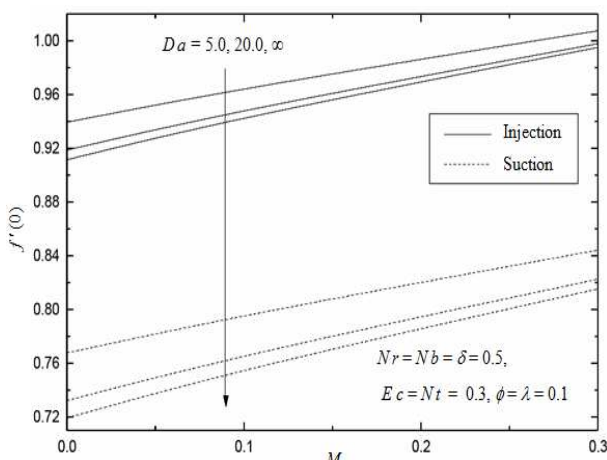


Fig. 8: Local skin Friction coefficient for various values of magnetic field parameter M and Darcy number Da

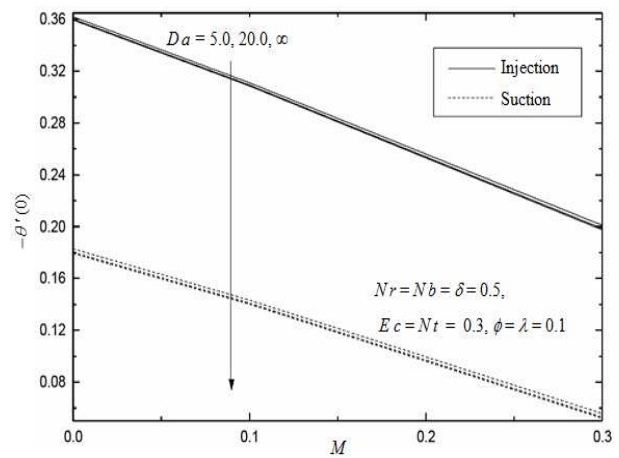


Fig. 9: Local Nusselt number for various values of magnetic field parameter M and Darcy number Da

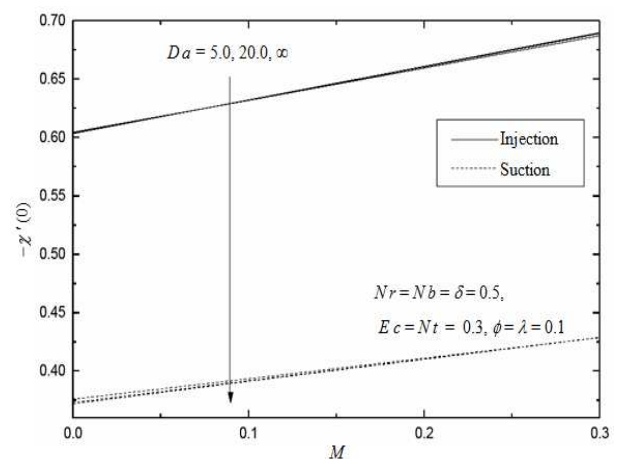


Fig. 10: Local Sherwood number for various values of magnetic field parameter M and Darcy number Da

When M , the magnetic field parameter, is increased, the local Sherwood number and skin friction coefficient both rise. In contrast, when fluid is constantly suctioned or injected, the local Nusselt number acts in the opposite way.

Figures 11, 12, 13 show how the Eckert number Ec affects the concentration, velocity, and temperature curves. From these numbers, it is evident that the fluid's velocity and temperature are both affected by the value of the Eckert number (Ec). In contrast, this increase in the Eckert number (Ec) results in a reduction in fluid concentration profiles for both injection and suction scenarios.

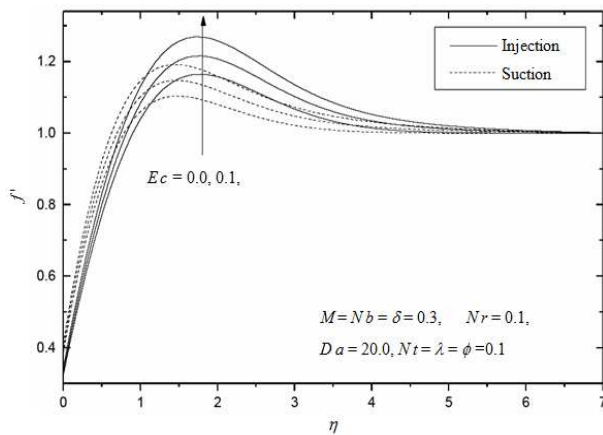


Fig. 11: Velocity profiles for various values of Eckert number Ec

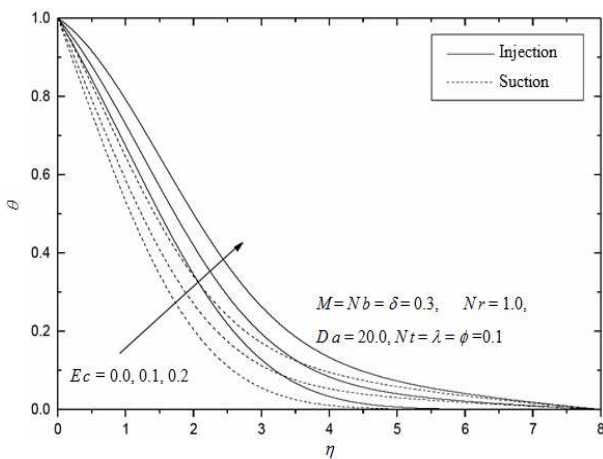


Fig. 12: Temperature profiles for various values of Eckert number Ec

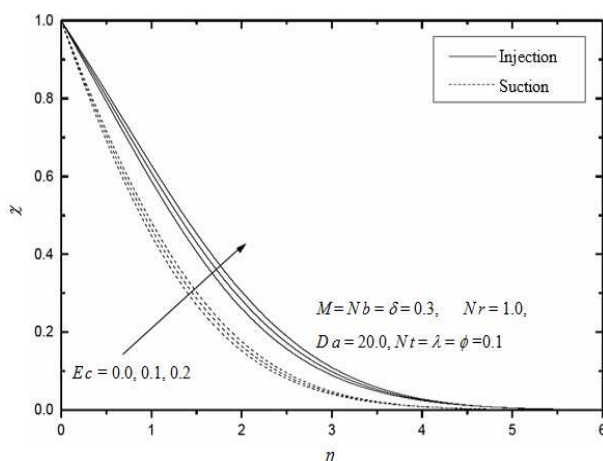


Fig. 13: Concentration profiles for various values of Eckert number Ec

thermophoresis parameter Nt and the Brownian motion number Nb , as shown in figures 14, 15, 16. All three of these numbers-the local skin friction coefficient, the local Nusselt number, and the local Sherwood number increase when the thermophoresis parameter Nt increases, as shown graphically. In contrast, when Nt grows, the local Nusselt number drops during injection and suction. Conversely, for injection and suction, a lower local Nusselt number and a higher local skin friction coefficient are produced by an increase in the Brownian motion number Nb , respectively. In contrast, when the Brownian motion number (Nb) rises in the suction case but falls in the injection scenario, the Sherwood number at the local level rises.

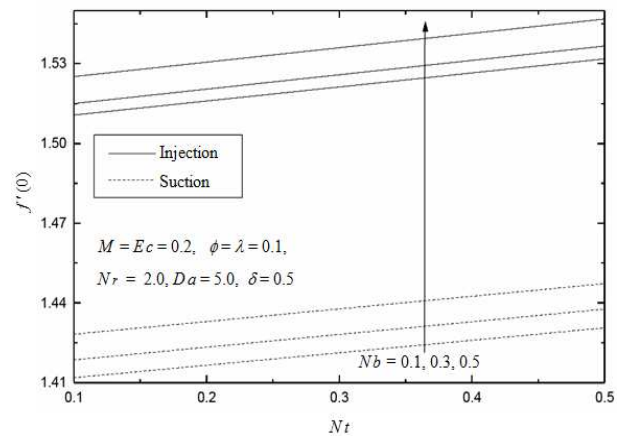


Fig. 14: Local skin Friction coefficient for various values of Brownian motion number Nb and thermophoresis parameter Nt

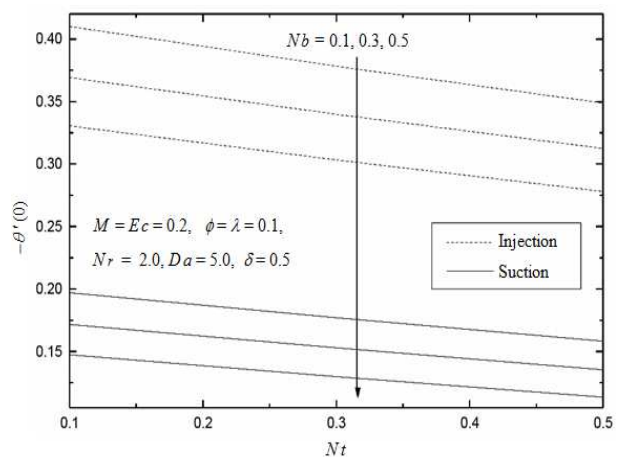


Fig. 15: Local Nusselt number for various values of Brownian motion number Nb and thermophoresis parameter Nt

Skin friction coefficient, Nusselt number, and Sherwood number at the local scale are affected by the

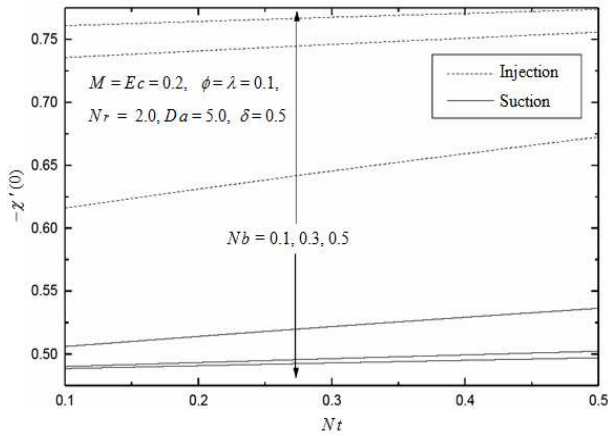


Fig. 16: Local Sherwood number for various values of Brownian motion number Nb and thermophoresis parameter Nt

Velocity, temperature, and concentration profiles are affected by the thermal buoyancy ratio parameter Nr , as shown in Figures 17, 18, 19.

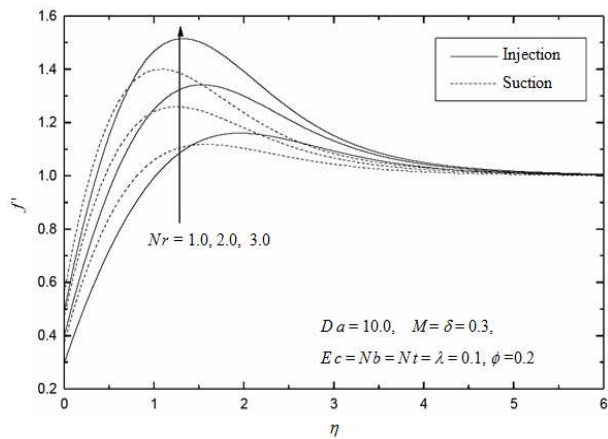


Fig. 17: Velocity profiles for various values of thermal buoyancy parameter Nr

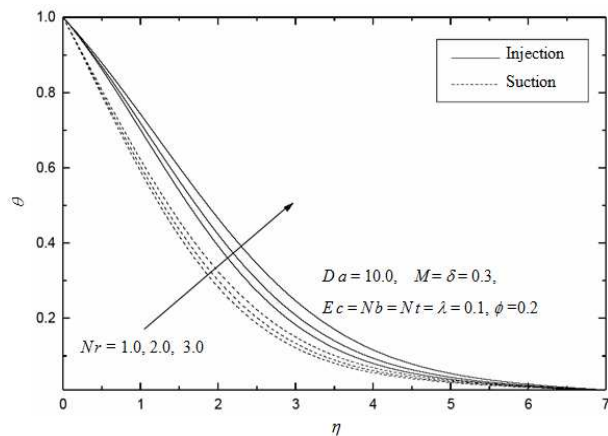


Fig. 18: Temperature profiles for various values of thermal buoyancy parameter Nr

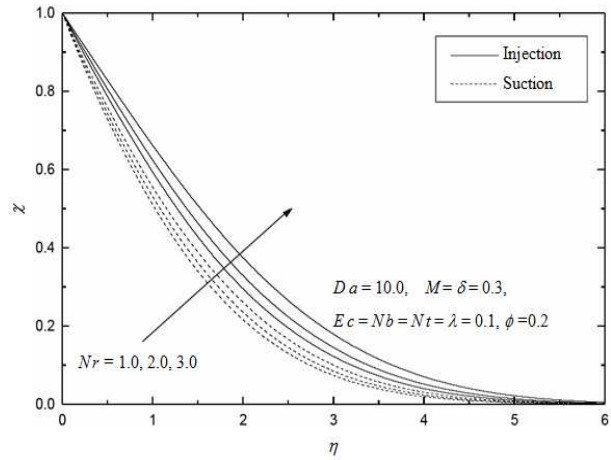


Fig. 19: Concentration profiles for various values of thermal buoyancy parameter Nr

Fluid temperature and concentration profiles for both continuous suction and injection decrease with increasing thermal buoyancy ratio parameter (Nr), according to these results. With this increment, nevertheless, the fluid's velocity grows.

For various values of the velocity slip parameter δ , the changes in the concentration, temperature, and velocity profiles are shown in Figures 20, 21, 22. The fluid's velocity grows in tandem with the velocity slip parameter (δ). The rise in the velocity slip parameter causes the nanofluid's movement to accelerate, which is the reason behind this. The introduction of slip into the nanofluid flow's trajectory causes this acceleration to take effect. Furthermore, whether the fluid is being injected or suctioned, the concentration and temperature both fall with increasing velocity slip parameter.

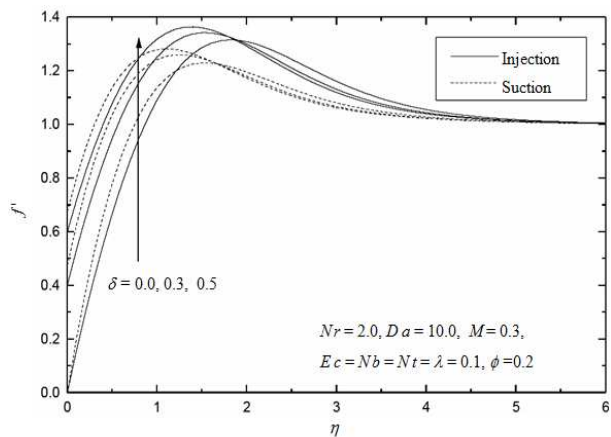


Fig. 20: Velocity profiles for various values of velocity slip parameter δ

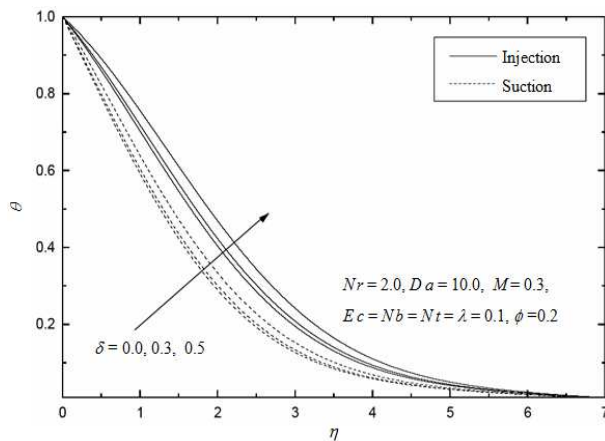


Fig. 21: Temperature profiles for various values of velocity slip parameter δ

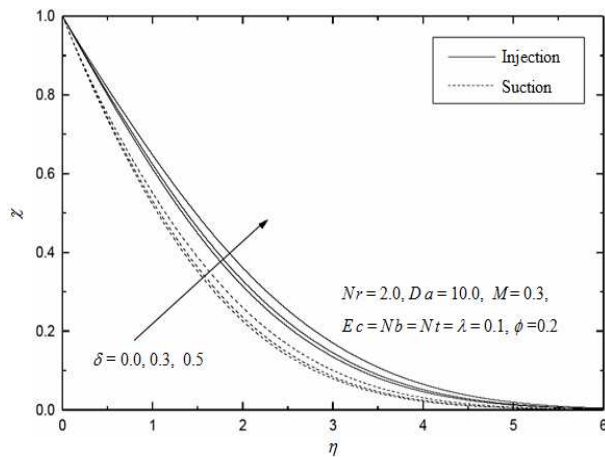


Fig. 22: Concentration profiles for various values of velocity slip parameter δ

5 Conclusions

The effect of viscous dissipation and Joule heating on mass and heat transfer in mixed convection in a boundary layer flow of an electrically conducting viscous incompressible nanofluid was investigated in this study. A magnetic field, velocity slip, suction, and injection through a porous media were all factors taken into account in the experiment. Utilizing suitable transformations, the governing equations are converted into comparable boundary layer equations. Subsequently, Runge-Kutta numerical integration and the shooting approach are employed for their solution.

- Visual representations of the effects of all flow-controlling parameters were provided in respect to concentration, temperature, and velocity, in addition to the local skin friction coefficient, Nusselt number, and Sherwood number.

- It turned out that raising the magnetic field parameter M makes the fluid move faster and hotter and lowers its concentration.
- All three local skin friction coefficients, local Nusselt and local Sherwood, could be reduced by raising Darcy number (Da) in the study, whether the fluid was constantly suctioned or injected.
- Whether the fluid is being suctioned or injected, a decrease in the fluid’s temperature and concentration profiles results from an increase in the thermal buoyancy ratio parameter Nr . Nevertheless, as Nr rises, the fluid’s velocity also increases.
- The research showed that fluid velocity increases with increasing velocity slip parameter δ , whilst temperature and concentration decrease. This is valid in the case of both injection and steady fluid suction.
- It was shown that while the fluid’s temperature and velocity both rise with an increasing Eckert number (Ec), the concentration profiles fall. Injection and suction scenarios are identical in this regard.

Author Contributions

M. M. M. Abdou: Conceptualization, Formal analysis, Methodology, Software, Validation, Writing-original draft.

R. M. M. AL-Wtheeh: Conceptualization, Formal analysis, Methodology, Software, Validation, Writing-original draft. Data Availability Statement.

All data used to support the findings of this study are included within the article.

Conflicts of Interest

The authors declare no conflict of interest.

Funding

This research received no external funding.

Acknowledgement

This study is supported via funding from Prince Sattam Bin Abdulaziz University project number (PSAU/2024/R/1445)

The authors express their gratitude to the anonymous referee who reviewed the manuscript thoroughly and provided insightful criticism that enhanced the final product.

References

- [1] W. Duangthongsuk and S. Wongwises, Effect of thermo physical properties models on the predicting of the convective heat transfer coefficient for low concentration nanofluid, *Int. Comm. Heat and Mass Transfer* **35**, 1320-1326, (2008).
- [2] J. A., Eastman, S. U. S. Choi, S. Li, L. J. Thompson and S. Lee, Enhanced thermal conductivity through the development of nanofluids, in; 1996 Fall Meeting of the Materials Research Society (MRs), Boston, USA, 3-11, (1996).
- [3] S. Lee and S. U. S. Choi, Application of metallic nanoparticle suspensions in advanced cooling systems, in: 1996 International Mechanical Engineering Congress and Exhibition, Atlanta, USA, (1996).
- [4] X. W. Wang, X. F. Xu and S. U. S. Choi, Thermal conductivity of nanoparticle-fluid mixture, *J. Thermophys. Heat Transfer*, **13**, 474-480, (1999).
- [5] S. Lee, S. U. S. Choi, S. Li and J. A. Eastman, Measuring thermal conductivity of fluids containing oxide nanoparticles, *J. Heat Transfer*, **121**, 280-289, (1999).
- [6] Y. Xuan and Q. Li, Heat transfer enhancement of nanofluids, *Int. J. Heat Fluid Flow*, **21**, 58-64, (2000).
- [7] Y. Xuan and W. Roetzel, Conceptions for heat transfer correlation of nanofluids, *Int. J. Heat Mass Transfer*, **43**, 3701-3707, (2000).
- [8] N. Bachok, A. Ishak and I. Pop, Boundary-layer flow of nanofluids over a moving surface in a flowing fluid, *Int. J. of Thermal Science*, **49**(9), pp. 1663-1668, (2010).
- [9] A. J. Chamkha and A. M. Aly, MHD free convection flow of a nano-fluid past a vertical plate in the presence of heat generation or absorption effects, *Chemical Engineering Communications*, **198**(3), 425-441, (2010).
- [10] W. A. Khan and I. Pop, Boundary-layer flow of a nanofluid past a stretching sheet, *Int. J. of Heat and Mass Transfer*, **53**(11-12), 2477-2483, (2010).
- [11] A. V. Kuznetsov and D. A. Nield, Natural convective boundary-layer flow of a nanofluid past a vertical plate, *Int. J. of Thermal Sciences* **49**(2), 243-247, (2010).
- [12] R. S. R. Gorla and A. Chamkha, Natural Convective Boundary Layer Flow over a Horizontal Plate Embedded in a Porous Medium Saturated with a Nanofluid, *Journal of Modern Physics*, **02**(02), 62-71, (2011), <https://doi.org/10.4236/JMP.2011.22011>
- [13] A. J. Chamkha and A. M. Rashad, Natural convection from a vertical permeable cone in a nanofluid saturated porous media for uniform heat and nanoparticles volume fraction fluxes, *Int. J. of Numerical Methods for Heat & Fluid Flow*, **22**(8), 1073-1085, (2012).
- [14] R. M. Rashad, M. A. El-Hakiem and M. M. M. Abdou, Natural convection boundary layer of a non-Newtonian fluid about a permeable vertical cone embedded in a porous medium saturated with a nanofluid, *Computers & Mathematics with Applications*, **62**(8), 3140-3151, (2011).
- [15] A. M. Rashad, Natural convection boundary layer flow along a sphere embedded in a porous medium filled with a nanofluid, *Latin American applied research*, **44**(2), 149-157, (2014).
- [16] D. Srinivasacharya and P. V. Kumar, Free Convection of a Nanofluid over an Inclined Wavy Surface Embedded in a Porous Medium with Wall Heat Flux, *Procedia Engineering*, **127**, pp. 40-47, (2015), <https://doi.org/10.1016/J.PROENG.2015.11.322>.
- [17] J. C. Umavathi, O. Ojjela, and K. Vajravelu, Numerical analysis of natural convective flow and heat transfer of nanofluids in a vertical rectangular duct using Darcy-Forchheimer-Brinkman model, *International Journal of Thermal Sciences*, **111**, 511-524, (2017), <https://doi.org/10.1016/j.ijthermalsci.2016.10.002>.
- [18] A. M. Rashad, A. J. Chamkha and M. M. M. Abdou, Mixed convection flow of non-Newtonian fluid from vertical surface saturated in a porous medium filled with a nanofluid, *J. of Applied Fluid Mechanics (JAFM)*, **6**(2), 301-309, (2013).
- [19] A. M. Rashad, A. J. Chamkha and M. Modather, Mixed convection boundary-layer flow past a horizontal circular cylinder embedded in a porous medium filled with a nanofluid under convective boundary condition, *Computers & Fluids* **86**, 380-388, (2013).
- [20] A. Abdulkadhim, H. K. Hamzah, F. H. Ali, C. Yıldız, A. M. Abed, E. M. Abed and M. Arici, Effect of heat generation and heat absorption on natural convection of Cu-water nanofluid in a wavy enclosure under magnetic field, *International Communications in Heat and Mass Transfer*, **120**, (2021), <https://doi.org/10.1016/j.icheatmasstransfer.2020.105024>.
- [21] M. A. Medebber, A. Aissa, M. E. A. Slimani and N. Retiel, Numerical study of natural convection in vertical cylindrical annular enclosure filled with Cu-water nanofluid under magnetic fields, *Defect and Diffusion Forum*, **392**, (2019), <https://doi.org/10.4028/www.scientific.net/DDF.392.123>.
- [22] M. M. Junoh, F. M. Ali and I. Pop, Magnetohydrodynamics stagnation-point flow of a nanofluid past a stretching/shrinking sheet with induced magnetic field: A revised model, *Symmetry*, **11**(9), (2019), <https://doi.org/10.3390/sym11091078>.
- [23] M. M. Junoh, F. M. Ali and I. Pop, MHD stagnation-point flow of a nanofluid past a stretching/shrinking sheet with induced magnetic field, *Journal of Engineering and Applied Sciences*, **13**(24), (2018), <https://doi.org/10.3923/jeasci.2018.10474.10481>.
- [24] F. Berrahil, A. Filali, C. Abid, S. Benissaad, R. Bessaih, R., and O. Matar, Numerical investigation on natural convection of Al₂O₃/water nanofluid with variable properties in an annular enclosure under magnetic field, *International Communications in Heat and Mass Transfer*, **126**, (2021), <https://doi.org/10.1016/j.icheatmasstransfer.2021.105408>.
- [25] K. Das, A. Sarkar and P. K. Kundu, Cu-water nanofluid flow induced by a vertical stretching sheet in presence of a magnetic field with convective heat transfer, *Propulsion and Power Research*, **6**(3), (2017), <https://doi.org/10.1016/j.jprr.2017.07.001>.
- [26] A. Raisi and A. Qanbary, Effect of magnetic field on forced convection between two nanofluid laminar flows in a channel, *Chinese Journal of Mechanical Engineering (English Edition)*, **29**(6), (2016), <https://doi.org/10.3901/CJME.2016.0615.072>
- [27] M. Ferdows, S. O. Adesanya, F. Alzahrani and T. A. Yusuf, Numerical investigation of a boundary layer water-based nanofluid flow with induced magnetic field, *Physica A: Statistical Mechanics and Its Applications*, **570**, (2021), <https://doi.org/10.1016/j.physa.2020.125492>.
- [28] M. Sheikholeslami, R. Ellahi and K. Vafai, Study of Fe₃O₄-water nanofluid with convective heat transfer in the presence

- of magnetic source, *Alexandria Engineering Journal*, **57**(2), (2018), <https://doi.org/10.1016/j.aej.2017.01.027>.
- [29] K. Hriczó, Boundary Value Problem for a Heated Nanofluid Flow in the Presence of Magnetic Field, *International Journal of Engineering and Management Sciences*, **4**(1), (2019), <https://doi.org/10.21791/ijems.2019.1.8>.
- [30] M. Sheikholeslami and D. D. Ganji, Nanofluid Flow and Heat Transfer in the Presence of Constant Magnetic Field, In *Applications of Nanofluid for Heat Transfer Enhancement*, (2017), <https://doi.org/10.1016/b978-0-08-102172-9.00006-x>.
- [31] M. Sheikholeslami and D. D. Ganji, Nanofluid Flow and Heat Transfer in the Presence of Variable Magnetic Field, In *Applications of Nanofluid for Heat Transfer Enhancement*, (2017), <https://doi.org/10.1016/b978-0-08-102172-9.00007-1>.
- [32] B. Sun, Y. Guo, D. Yang, D. and H. Li, The effect of constant magnetic field on convective heat transfer of Fe₃O₄/water magnetic nanofluid in horizontal circular tubes, *Applied Thermal Engineering*, **171**, (2020), <https://doi.org/10.1016/j.applthermaleng.2020.114920>.
- [33] M. S. Krakov and I. V. Nikiforov, Natural convection in a horizontal cylindrical enclosure filled with a magnetic nanofluid: Influence of the uniform outer magnetic field, *International Journal of Thermal Sciences*, **133**, (2018), <https://doi.org/10.1016/j.ijthermalsci.2018.07.010>.
- [34] M. Hajiyan, S. Mahmud, M. Biglarbegian, H. A. Abdullah and A. Chamkha, Effect of magnetic field-dependent thermal conductivity on natural convection of magnetic nanofluid inside a square enclosure, *International Journal of Numerical Methods for Heat and Fluid Flow*, **29**(4), (2019), <https://doi.org/10.1108/HFF-07-2018-0374>.
- [35] A. S. P. Devi and B. Ganga, Effects of viscous and joules dissipation on MHD flow, heat and mass transfer past a stretching porous surface embedded in a porous medium, *Nonlinear Analysis: Modelling and Control*, **14**(3), 303-314, (2009), <https://doi.org/10.15388/NA.2009.14.3.14497>.
- [36] B. Ganga, S. M. Y. Ansari, N. V. Ganesh and A. K. Abdul Hakeem, MHD radiative boundary layer flow of nanofluid past a vertical plate with internal heat generation/absorption, viscous and ohmic dissipation effects, *Journal of the Nigerian Mathematical Society*, **34**(2), 181-194, (2015), <https://doi.org/10.1016/J.JNNMS.2015.04.001>.
- [37] F. Mabood, W. A. Khan A. I. M. Ismail, MHD boundary layer flow and heat transfer of nanofluids over a nonlinear stretching sheet: A numerical study, *Journal of Magnetism and Magnetic Materials*, **374**, 569-576, (2015), <https://doi.org/10.1016/j.jmmm.2014.09.013>.
- [38] T. Hayat, M. Imtiaz and A. Alsaedi, Melting heat transfer in the MHD flow of Cu-water nanofluid with viscous dissipation and Joule heating, *Advanced Powder Technology*, **27**(4), 1301-1308, (2016), <https://doi.org/10.1016/j.apt.2016.04.024>.
- [39] A. K. Pandey and M. Kumar, Effect of viscous dissipation and suction/ injection on MHD nanofluid flow over a wedge with porous medium and slip, *Alexandria Engineering Journal*, **55**(4), 3115-3123, (2016), <https://doi.org/10.1016/j.aej.2016.08.018>.
- [40] P. Besthapu, R. U. Haq, S. Bandari and Q. M. Al-Mdallal, Mixed convection flow of thermally stratified MHD nanofluid over an exponentially stretching surface with viscous dissipation effect, *Journal of the Taiwan Institute of Chemical Engineers*, **71**, 307-314, (2017), <https://doi.org/10.1016/J.JTICE.2016.12.034>.
- [41] H. Upreti, A. K. Pandey and M. Kumar, MHD flow of Ag-water nanofluid over a flat porous plate with viscous-Ohmic dissipation, suction/injection and heat generation /absorption, *Alexandria Engineering Journal*, Vol. **57**(3), 1839-1847, (2018), <https://doi.org/10.1016/J.AEJ.2017.03.018>.
- [42] D. Gopal, S. Jagadha, P. Sreehari, N. Kishan and D. Mahendar, A numerical study of viscous dissipation with first order chemical reaction and ohmic effects on MHD nanofluid flow through an exponential stretching sheet, *Materials Today: Proceedings*, **59**, 1028-1033, (2022), <https://doi.org/10.1016/J.MATPR.2022.02.368>.
- [43] M. R. Khan, S. Mao, W. Deebani and A. M. A. Elsidieq, Numerical analysis of heat transfer and friction drag relating to the effect of Joule heating, viscous dissipation, and heat generation/absorption in aligned MHD slip flow of a nanofluid, *International Communications in Heat and Mass Transfer*, **131**, 105843, (2022), <https://doi.org/10.1016/J.ICHEATMASSTRANSFER.2021.105843>.
- [44] F. Ahmed, M. Iqbal and N. S. Akbar, Viscous dissipation and joule heating effects on forced convection power law fluid flow through annular duct, *Proceedings of the Institution of Mechanical Engineers, Part C: Journal of Mechanical Engineering Science*, **235**(21), 5858-5865, (2021).
- [45] B. K. Swain, B. C. Parida, S. Kar and N. Senapati, Viscous dissipation and joule heating effect on MHD flow and heat transfer past a stretching sheet embedded in a porous medium, *Heliyon*, **6**, (2020), e05338.
- [46] M. R. Khan, V. Puneeth, M. K. Alaoui, R. Alrobaea and M. M. M. Abdou, Heat transfer in a dissipative nanofluid passing by a convective stretching/ shrinking cylinder near the stagnation point, *Z Angew Math Mech.*, (2023), e202300733., <https://doi.org/10.1002/zamm.202300733>.
- [47] O. D. Makinde and I. L. Animasaun, Thermophoresis and Brownian motion effects on MHD bioconvection of nanofluid with nonlinear thermal radiation and quartic chemical reaction past an upper horizontal surface of paraboloid of revolution, *J. Mol. Liq.*, **221**, pp. 733-743, (2016), <https://doi.org/10.1016/j.molliq.2016.06.047>.
- [48] H. T. Lin and L. K. Lin, Similarity solutions for laminar forced convection heat transfer from wedges to fluids of any Prandtl number, *Int. J. Heat Mass Transfer*, **30**, 1111-1118, (1987).
- [49] K. A. Yih, MHD forced convection flow adjacent to a non-isothermal wedge, *Int. Commun. Heat Mass*, **26**, 819-827, (1999).
- [50] A. J. Chamkha, M. Mujtaba, A. Quadri and C. Issa, Thermal radiation effects on MHD forced convection flow adjacent to a non-isothermal wedge in the presence of heat source or sink, *Heat Mass Transfer*, **39**, 305-312, (2003).
- [51] D. A. Nield and A. V. Kuznetsov, Boundary layer analysis of forced convection with a plate and porous substrate, *Acta Mech.*, **166**, 141-148, (2003).
- [52] A. V. Kuznetsov and D. A. Nield, Boundary layer treatment of forced convection over a wedge with an attached porous substrate, *J. Porous Media*, **9**(7), 683-694, (2006).
- [53] N. W. Saeid, Mixed convection flow along a vertical plate subjected to time-periodic surface temperature oscillations, *Int. J. Therm. Sci.*, **44**, 531- 539, (2005).

- [54] T. Watanabe and I. Pop, Thermal boundary layers in magnetohydrodynamic flow over a flat plate in the presence of a transverse magnetic field, *Acta Mech.*, **105**, 233-238, (1994).
- [55] O. Aydın and A. Kaya, MHD mixed convection of a viscous dissipating fluid about a permeable vertical flat plate, *Applied Mathematical Modelling*, **33**, 4086-4096, (2009).
- [56] H. A. Nabwey, S. M. M. EL-Kabeir, A. M. Rashad and M. M. M. Abdou, Gyrotactic micro-organisms mixed convection flow of nanofluid over a vertically surfaced saturated porous media, *Alexandria Engineering Journal*, **61**(3), 1804-1822, (2022), <https://doi.org/10.1016/J.AEJ.2021.06.080>.
-

Mohammed Modather Mohammed Abdou is Professor of Mathematics in College of Science & Humanity Studies, Prince Sattam Bin Abdulaziz University in Alkharj, Department of Mathematics, Faculty of Science, Aswan University, Egypt.

Refah Mohammed Masfar Al Wtheeh is Bachelor of Science in Mathematics from College of Science and Humanity Studies in Alkharj. Now Master's Student in department of Mathematics, College of Science & Humanity Studies, Prince Sattam Bin Abdulaziz University in Alkharj.